

Power Corrections to Event Shapes in Deep Inelastic Scattering*

M. Dasgupta and B.R. Webber
Cavendish Laboratory, University of Cambridge,
Madingley Road, Cambridge CB3 0HE, U.K.

Abstract

We investigate the power-suppressed corrections to the mean values of various quantities that characterise the shapes of final states in deep inelastic lepton scattering. Our method is based on an analysis of one-loop Feynman graphs containing a massive gluon, which is equivalent to the evaluation of leading infrared renormalon contributions. As in e^+e^- annihilation, we find that the leading corrections are proportional to $1/Q$. We give quantitative estimates based on the hypothesis of a universal low-energy effective coupling.

Cavendish-HEP-96/5
April 1997

*Research supported in part by the U.K. Particle Physics and Astronomy Research Council and by the EC Programme “Training and Mobility of Researchers”, Network “Hadronic Physics with High Energy Electromagnetic Probes”, contract ERB FMRX-CT96-0008.

1 Introduction

The study of final-state properties in deep inelastic lepton scattering (DIS) has received a great impetus from the increasing quantity and kinematic range of the HERA data. The determination of the strong coupling α_s from final-state properties in DIS is an attractive possibility because of the relative simplicity of the lepton-hadron interaction, combined with the wide range of dynamical scales available in a single experiment at a single beam energy. It is expected that the scale for α_s will be set primarily by the lepton-hadron momentum transfer-squared Q^2 , which can range from zero to 10^5 GeV^2 at HERA. Thus there should be a wide region in which the value and running of $\alpha_s(Q^2)$ can be observed with good precision.

One possible method for α_s determination is the measurement of jet fractions [1], defined according to one of the several available infrared-safe jet algorithms [2,3]. By definition, jet rates defined by an infrared-safe algorithm can be computed in perturbation theory, and next-to-leading-order calculations are now available [4,5]. The α_s values obtained by comparing jet rates with HERA data are consistent with those found in other processes, and in particular they show the expected decrease with increasing Q^2 .

In the present paper we consider a different set of DIS final-state observables which can be used to determine α_s . These are the various *event shape variables* which can be defined in analogy with those used in the study of e^+e^- annihilation final states. In e^+e^- physics, event shapes have been found to be a useful tool for testing QCD and measuring α_s . They can be defined so as to be sensitive to different aspects of QCD dynamics (e.g. the longitudinal or transverse development of jets) are subject to different non-perturbative ‘hadronization’ corrections. Thus α_s determinations from a variety of event shapes complement those from jet rates and give an indication of the systematic uncertainties due to non-perturbative effects. The same considerations make it important to calculate and measure event shapes in DIS.

Another reason to measure event shapes is that there are new theoretical ideas about non-perturbative corrections to them [6–10], which provide constraints on α_s determinations from event shapes and are interesting to test in their own right. By looking at the behaviour of the QCD perturbation series in high orders, one can identify unsummable, factorially divergent sets of contributions (infrared renormalons [11]) which indicate that non-perturbative power-suppressed corrections must be included. The Q^2 -dependence of the leading correction to a given quantity can be inferred, and by making further universality assumptions one may also estimate its magnitude. Tests of these ideas provide information on the transition from the perturbative to the non-perturbative regime in QCD. In particular, one can investigate the possibility that an approximately universal low-energy effective coupling may be a useful phenomenological concept [7,8,12].

Such an approach has been applied with some success to e^+e^- event shapes [7,8,13] and fragmentation functions [14], and to DIS structure functions [8,15]. In the present paper we extend it to event shapes in DIS [16]. We find that, as in e^+e^- annihilation, the leading power corrections to these quantities are typically proportional to $1/Q$. The hypothesis that they are related to a universal low-energy effective coupling implies that their magnitudes are given by a single non-perturbative parameter. We give quantitative estimates based on the value of this parameter derived from e^+e^- data.

In the following Section we explain how the DIS event shape variables that we compute are defined. In Sect. 3 we give the leading-order perturbative predictions for these quantities. To determine α_s , one needs the predictions in next-to-leading order, which are not yet available. However, the leading-order calculation provides a useful guide to the relative importance of the power-suppressed corrections, which we estimate in Sect. 4 using the method of Ref. [8]. We explain how these estimates can be refined and combined with the next-to-leading predictions when they become available. Finally, our results are summarized briefly in Sect. 5.

2 Event shape variables in DIS

A complication in DIS, absent from e^+e^- annihilation, is the presence in the final state of the remnant of the initial-state hadron, i.e. the constituents that did not participate in the hard scattering of the lepton. It is expected that the fragmentation of the remnant will be dominated by soft, non-perturbative physics. While of interest for studying the hadronization process, the remnant fragmentation is not so useful for α_s determinations, and therefore we concentrate here on aspects of event shapes that are not sensitive to it. This is conveniently done by looking at the final state in the *Breit frame of reference* [17,18,19].

We consider the deep inelastic scattering of a lepton of momentum l from a nucleon of momentum P , with momentum transfer q . The main kinematic variables are $Q^2 = -q^2$, the Bjorken variable $x = Q^2/2P \cdot q$ and $y = P \cdot q/P \cdot l \simeq Q^2/xs$, s being the total c.m. energy squared. Then the Breit frame is the rest-frame of $2xP + q$. In this frame the momentum transfer q is purely spacelike, and we choose to align it along the $+z$ axis:

$$P = \frac{1}{2}Q(1/x, 0, 0, -1/x), \quad q = \frac{1}{2}Q(0, 0, 0, 2). \quad (2.1)$$

To a good approximation, the fragmentation products of the remnant will be moving in directions close to that of the incoming nucleon, i.e. they will remain in the ‘remnant hemisphere’ H_r ($p_z < 0$). On the other hand the products of the hard lepton scattering will tend to be found in the ‘current hemisphere’ H_c ($p_z > 0$). In fact in the parton model the scattered parton moves along the current ($+z$) axis with momentum $xP + q = \frac{1}{2}Q(1, 0, 0, 1)$. Thus in the parton model the current hemisphere looks like one hemisphere of the final state in e^+e^- annihilation at centre-of-mass energy Q . Fragmentation studies have shown that this similarity is indeed manifest in hadron spectra and multiplicities [20]. This makes it natural to define event shape variables in close analogy to those for e^+e^- annihilation, but limited to particles a appearing in the current hemisphere, $a \in H_c$.

We can now construct infrared-safe quantities that characterize the shape of the event defined in this way. Perhaps the simplest is the *current jet thrust* [17]

$$T_Q = 2 \sum_{a \in H_c} \mathbf{p}_a \cdot \mathbf{n} / Q \quad (2.2)$$

where \mathbf{n} represents the unit 3-vector along the current direction (the $+z$ axis, in our convention). The subscript Q indicates that T is normalized to $\frac{1}{2}Q$. Alternatively we may normalize to the total energy in the current hemisphere,

$$T_E = \sum_{a \in H_c} \mathbf{p}_a \cdot \mathbf{n} / \sum_{a \in H_c} E_a. \quad (2.3)$$

Both of these quantities are equal to unity in the Born approximation, and their deviation from this value measures the longitudinal development of the current jet. It will therefore be convenient to study instead the quantities $\tau_Q = 1 - T_Q$ and $\tau_E = 1 - T_E$, which vanish in the Born approximation.

It is kinematically possible for the Breit frame current hemisphere to be empty. In that case, taken literally, Eq. (2.2) implies that $T_Q = 0$, hence $\tau_Q = 1$, while Eq. (2.3) leaves τ_E undefined. For consistency with the other event shapes defined below, we instead define $\tau_Q = \tau_E = 0$ when the current hemisphere is empty.

Similarly we can define the *current jet broadening* [21]

$$B_Q = \sum_{a \in H_c} |\mathbf{p}_a \times \mathbf{n}| / Q, \quad (2.4)$$

or

$$B_E = \frac{1}{2} \sum_{a \in H_c} |\mathbf{p}_a \times \mathbf{n}| / \sum_{a \in H_c} E_a, \quad (2.5)$$

which emphasizes the transverse development of the jet.

Both the thrust and the broadening are defined here with respect to the current direction \mathbf{n} . Two quantities which measure the jet development independent of direction (apart from the restriction to particles in the current hemisphere) are the scaled *current jet mass*

$$\rho_Q = \left(\sum_{a \in H_c} p_a \right)^2 / Q^2 \quad (2.6)$$

and the *C-parameter* [22]

$$C_Q = 3(\lambda_1 \lambda_2 + \lambda_2 \lambda_3 + \lambda_3 \lambda_1) \quad (2.7)$$

where $\lambda_{1,2,3}$ are the eigenvalues of the linearized momentum tensor

$$\Theta^{ij} = 2 \sum_{a \in H_c} (\mathbf{p}_a^i \mathbf{p}_a^j / |\mathbf{p}_a|) / Q. \quad (2.8)$$

Again, we may alternatively define quantities ρ_E and C_E , in which Q is replaced by twice the total energy in the current hemisphere, so that

$$\rho_E / \rho_Q = C_E / C_Q = Q^2 / \left(2 \sum_{a \in H_c} E_a \right)^2. \quad (2.9)$$

3 Leading-order perturbation theory

At first order in α_s , up to two final-state partons can be emitted in the hard lepton-parton subprocess, as illustrated in Fig. 1. The momentum of the struck parton is $p = xP/\xi$ ($x < \xi < 1$) and we define $z = P \cdot r / P \cdot q$ ($0 < z < 1$).

The differential cross section is

$$\frac{d^3\sigma}{dx dQ^2 dz} = \frac{2\pi\alpha^2}{Q^4} \left\{ [1 + (1-y)^2] F_T(x, z) + 2(1-y) F_L(x, z) \right\}. \quad (3.1)$$

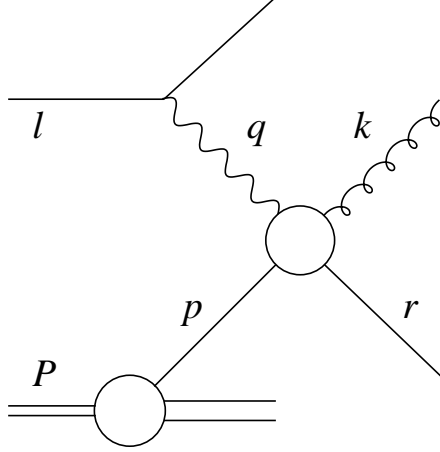


Figure 1: Jet production in deep inelastic scattering.

The generalized transverse and longitudinal structure functions $F_T(x, z) = 2F_1(x, z)$ and $F_L(x, z) = F_2(x, z)/x - 2F_1(x, z)$ are of the form (for $z < 1$)

$$F_i(x, z) = \frac{\alpha_s}{2\pi} \int_x^1 \frac{d\xi}{\xi} [C_F C_{i,q}(\xi, z) q(x/\xi) + T_f C_{i,g}(\xi, z) g(x/\xi)] \quad (3.2)$$

where

$$q(x) = \sum_{j=1}^f e_j^2 [q_j(x) + \bar{q}_j(x)] , \quad T_f = T_R \sum_{j=1}^f e_j^2 \quad (3.3)$$

for f active quark flavours, $C_F = 4/3$, $T_R = 1/2$ and [18]

$$\begin{aligned} C_{T,q}(\xi, z) &= \frac{\xi^2 + z^2}{(1-\xi)(1-z)} + 2\xi z + 2 \\ C_{L,q}(\xi, z) &= 4\xi z \\ C_{T,g}(\xi, z) &= [\xi^2 + (1-\xi)^2] \frac{z^2 + (1-z)^2}{z(1-z)} \\ C_{L,g}(\xi, z) &= 8\xi(1-\xi) . \end{aligned} \quad (3.4)$$

In the Breit frame P and q are given by Eq. (2.1) and we can write

$$\begin{aligned} p &= \frac{1}{2}Q(1/\xi, 0, 0, -1/\xi) \\ r &= \frac{1}{2}Q(z_0, z_\perp, 0, z_3) \\ k &= \frac{1}{2}Q(\bar{z}_0, -z_\perp, 0, \bar{z}_3) \end{aligned} \quad (3.5)$$

where

$$\begin{aligned} z_0 &= 2z - 1 + (1-z)/\xi \\ z_3 &= 1 - (1-z)/\xi \\ \bar{z}_0 &= 1 - 2z + z/\xi \\ \bar{z}_3 &= 1 - z/\xi \\ z_\perp &= 2\sqrt{z(1-z)(1-\xi)/\xi} . \end{aligned} \quad (3.6)$$

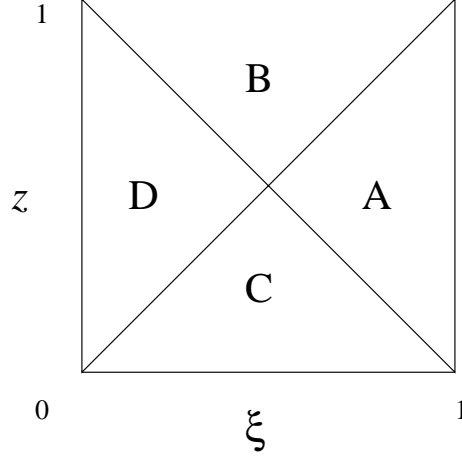


Figure 2: Phase space region for jet production in deep inelastic scattering.

We can distinguish four subregions of phase space, as illustrated in Fig. 2:

A: both produced parton momenta k, r in the current hemisphere ($z_3, \bar{z}_3 > 0$);

B: only parton momentum r in the current hemisphere ($z_3 > 0, \bar{z}_3 < 0$);

C: only parton momentum k in the current hemisphere ($z_3 < 0, \bar{z}_3 > 0$);

D: no produced parton momenta in the current hemisphere ($z_3, \bar{z}_3 < 0$).

In leading order the event shape variables defined in Sect. 2 are given in these regions by Table 1. By definition they are all zero in region D. By construction, they all vanish in the soft and/or collinear limits $\xi, z \rightarrow 1$. Note that ρ and C also vanish throughout regions B and C.

At any particular values of x and Q^2 , the mean value of a shape variable S is now given in leading order by

$$\langle S \rangle = \frac{2\pi\alpha^2}{Q^4} \int_0^1 dz \left\{ [1 + (1-y)^2] F_T^{(S)}(x) + 2(1-y) F_L^{(S)}(x) \right\} \Big/ \frac{d^2\sigma_0}{dx dQ^2} \quad (3.7)$$

where

$$F_i^{(S)}(x) = \frac{\alpha_s}{2\pi} \int_x^1 \frac{d\xi}{\xi} \int_0^1 dz S(\xi, z) [C_F C_{i,q}(\xi, z) q(x/\xi) + T_f C_{i,g}(\xi, z) g(x/\xi)] \quad (3.8)$$

and the denominator is the differential cross section evaluated in Born approximation,

$$\frac{d^2\sigma_0}{dx dQ^2} = \frac{2\pi\alpha^2}{Q^4} [1 + (1-y)^2] q(x) . \quad (3.9)$$

We discuss the numerical values of the leading-order predictions together with the power corrections in the following Section.

Table 1: Event shape variables $S(\xi, z)$ in leading order.

S	A	B	C
τ_Q	$(1 - \xi)/\xi$	$1 - z_3$	$1 - \bar{z}_3$
τ_E	$2(1 - \xi)$	$1 - z_3/z_0$	$1 - \bar{z}_3/\bar{z}_0$
B_Q	z_\perp	$z_\perp/2$	$z_\perp/2$
B_E	ξz_\perp	$z_\perp/2z_0$	$z_\perp/2\bar{z}_0$
ρ_Q	$(1 - \xi)/\xi$	0	0
ρ_E	$\xi(1 - \xi)$	0	0
C_Q	$3(2\xi - 1)^2 z_\perp^2 / \xi^2 z_0 \bar{z}_0$	0	0
C_E	$3(2\xi - 1)^2 z_\perp^2 / z_0 \bar{z}_0$	0	0

4 Power corrections

Our estimate of the leading power corrections to the perturbative results given above is based on the approach of Ref. [8]. Non-perturbative effects at long distances are assumed to give rise to a modification $\delta\alpha_{\text{eff}}(\mu^2)$ in the QCD effective coupling at low values of the scale μ^2 . The effect on some observable F is then given by a *characteristic function* $\mathcal{F}(x, \epsilon)$, as follows:

$$\delta F(x, Q^2) = \int_0^\infty \frac{d\mu^2}{\mu^2} \delta\alpha_{\text{eff}}(\mu^2) \dot{\mathcal{F}}(x, \epsilon = \mu^2/Q^2) \quad (4.1)$$

where

$$\dot{\mathcal{F}}(x, \epsilon) \equiv -\epsilon \frac{\partial}{\partial \epsilon} \mathcal{F}(x, \epsilon) . \quad (4.2)$$

The characteristic function is obtained by computing the relevant one-loop graphs with a non-zero gluon mass $\mu = Q\sqrt{\epsilon}$ [6,23].

Arbitrary finite modifications of the effective coupling at low scales would generally introduce power corrections of the form $1/\mu^{2p}$ into the ultraviolet behaviour of the running coupling α_s itself. Such a modification would destroy the basis of the operator product expansion [24]. One must therefore require that at least the first few integer moments of the coupling modification should vanish:

$$\int_0^\infty \frac{d\mu^2}{\mu^2} (\mu^2)^p \delta\alpha_{\text{eff}}(\mu^2) = 0 ; \quad p = 1, \dots, p_{\text{max}} . \quad (4.3)$$

The upper bound p_{max} could be set by instanton–anti-instanton contributions ($p_{\text{max}} \sim 9$). The constraint (4.3) means that only those terms in the small- ϵ behaviour of the characteristic function that are *non-analytic* at $\epsilon = 0$ will lead to power-behaved non-perturbative

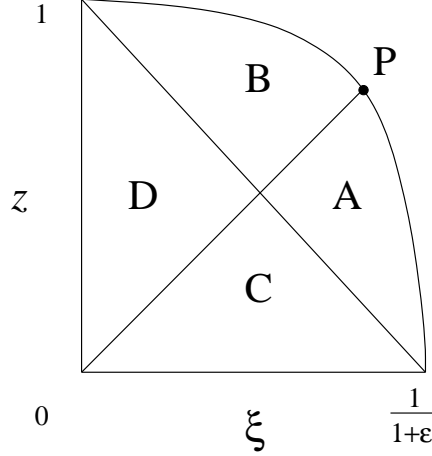


Figure 3: Phase space region with gluon mass-squared $\mu^2 = \epsilon Q^2$.

contributions. These are just the terms that give rise to infrared renormalons in perturbation theory [23].

For gluon mass-squared $\mu^2 = \epsilon Q^2$ the quark coefficient functions in Eq. (3.4) become

$$C_{T,q}(\xi, z, \epsilon) = \frac{(1-z)(1-\xi) + 2\xi z(1-z)^2 - \xi\epsilon}{(1-z-\xi\epsilon)^2} + \frac{2\xi z(1-\epsilon)}{(1-z-\xi\epsilon)(1-\xi)} + \frac{(1-z)(1-\xi) - \xi\epsilon}{(1-\xi)^2}$$

$$C_{L,q}(\xi, z, \epsilon) = \frac{4\xi z(1-z)^2}{(1-z-\xi\epsilon)^2} . \quad (4.4)$$

Processes involving an incoming gluon are not expected to give terms that are non-analytic at $\epsilon = 0$, and therefore we do not consider them as a source of power corrections. The kinematic variables that give the momenta according to Eq. (3.5) are now

$$\begin{aligned} z_0 &= 2z - 1 + (1-z)/\xi - \epsilon \\ z_3 &= 1 - (1-z)/\xi + \epsilon \\ \bar{z}_0 &= 1 - 2z + z/\xi + \epsilon \\ \bar{z}_3 &= 1 - z/\xi - \epsilon \\ z_\perp &= 2\sqrt{z(1-z)(1-\xi)/\xi - \epsilon z} . \end{aligned} \quad (4.5)$$

Thus the phase space region is now $0 < z < 1 - \epsilon\xi/(1-\xi)$, as illustrated in Fig. 3. The regions A, ... D defined above in terms of the signs of z_3 and \bar{z}_3 are as indicated.

The corresponding characteristic function for the mean value of some event shape variable S is given by Eq. (3.7) with $F_i^{(S)}(x)$ replaced by $(C_F/2\pi)\mathcal{F}_i^{(S)}(x, \epsilon)$ where

$$\mathcal{F}_i^{(S)}(x, \epsilon) = \int_x^1 \frac{d\xi}{\xi} \int_0^1 dz S(\xi, z, \epsilon) C_{i,q}(\xi, z, \epsilon) \Theta(1-z-\xi+\xi z-\epsilon\xi) q(x/\xi) . \quad (4.6)$$

Note that for brevity we have extracted the overall factor of $C_F/2\pi$. The expressions for the shape variables $S(\xi, z, \epsilon)$ are as given in Table 1, but with the kinematic variables now given by Eqs. (4.5) instead of Eqs. (3.6).

Finding the leading non-analytic term in the behaviour of the integral (4.6) as $\epsilon \rightarrow 0$, differentiating as instructed in Eq. (4.2), and inserting the result in Eq. (4.1), we obtain the corresponding predicted power correction. Generally speaking, the small- ϵ behaviour of the characteristic function is dominated by the region around the boundary point P in Fig. 3, and therefore the leading power correction is independent of whether we normalize the shape variable to $Q/2$ or to the energy in the current hemisphere.

Following Ref. [8], we may express the magnitudes of power corrections in terms of the moment integrals

$$A_{2p} = \frac{C_F}{2\pi} \int_0^\infty \frac{d\mu^2}{\mu^2} \mu^{2p} \delta\alpha_{\text{eff}}(\mu^2) , \quad (4.7)$$

which vanish for integer p , and their p -derivatives

$$A'_{2p} = \frac{C_F}{2\pi} \int_0^\infty \frac{d\mu^2}{\mu^2} \mu^{2p} \log \mu^2 \delta\alpha_{\text{eff}}(\mu^2) , \quad (4.8)$$

which are in general non-vanishing for any p . The leading corrections to the event shapes we are considering correspond to $p = \frac{1}{2}$, and therefore, on the assumption that $\delta\alpha_{\text{eff}}$ is universal, they can all be expressed in terms of the two non-perturbative parameters A_1 and A'_1 . Studies of event shapes in e^+e^- annihilation suggest that $A_1 \simeq 0.25$ GeV [8], with A'_1 as yet undetermined.

As an alternative representation of the magnitudes of power corrections, we may adopt the approach of Ref. [7] and express them directly in terms of moments of α_{eff} over the infrared region. We substitute for $\delta\alpha_{\text{eff}}$ in Eq. (4.7)

$$\delta\alpha_{\text{eff}}(\mu^2) \simeq \alpha_{\text{eff}}(\mu^2) - \alpha_s^{\text{PT}}(\mu^2) , \quad (4.9)$$

where α_s^{PT} represents the expression for α_s corresponding to the part already included in the perturbative prediction. As discussed in Ref. [7], if the perturbative calculation is carried out to second order in the $\overline{\text{MS}}$ renormalization scheme, with renormalization scale μ_R^2 , then we have

$$\alpha_s^{\text{PT}}(\mu^2) = \alpha_s(\mu_R^2) + [b \ln(\mu_R^2/\mu^2) + k] \alpha_s^2(\mu_R^2) \quad (4.10)$$

where ($C_A = 3$)

$$b = \frac{11C_A - 2f}{12\pi} , \quad k = \frac{(67 - 3\pi^2)C_A - 10f}{36\pi} . \quad (4.11)$$

The constant k comes from a change of scheme from $\overline{\text{MS}}$ to the more physical scheme [25] in which α_{eff} is defined. Then above some infrared matching scale μ_1 we assume that $\alpha_{\text{eff}}(\mu^2)$ and $\alpha_s^{\text{PT}}(\mu^2)$ approximately coincide, so that

$$\begin{aligned} A_1 &\simeq \frac{C_F}{2\pi} \int_0^{\mu_1^2} \frac{d\mu^2}{\mu^2} \mu \left(\alpha_{\text{eff}}(\mu^2) - \alpha_s(\mu_R^2) - [b \ln(\mu_R^2/\mu^2) + k] \alpha_s^2(\mu_R^2) \right) \\ &= \frac{C_F}{\pi} \mu_1 \left(\bar{\alpha}_0(\mu_1) - \alpha_s(\mu_R^2) - [b \ln(\mu_R^2/\mu_1^2) + k + 2b] \alpha_s^2(\mu_R^2) \right) , \end{aligned} \quad (4.12)$$

where

$$\bar{\alpha}_0(\mu_1) \equiv \frac{1}{\mu_1} \int_0^{\mu_1} \alpha_{\text{eff}}(\mu^2) d\mu . \quad (4.13)$$

Thus in this notation the value of A_1 determines the average value of the effective coupling below the matching scale μ_1 . The dependence of $\bar{\alpha}_0$ on μ_1 is partially compensated by the

μ_I -dependence of the other terms on the right-hand side of Eq. (4.12). The dependence on the renormalization scale μ_R^2 should help to compensate the scale dependence of the perturbative part. Notice that if we take $\mu_R^2 \propto Q^2$ then A_1 has a logarithmic dependence on Q^2 . In general we do expect ‘power’ corrections to have additional logarithmic Q^2 -dependence (anomalous dimensions), but this cannot yet be calculated reliably for event shapes.

In Ref. [7] it was found that the formula (4.12) with $\mu_R^2 = Q^2$, $\mu_I = 2 \text{ GeV}$ and $\bar{\alpha}_0(2 \text{ GeV}) = 0.52$ gave good agreement with e^+e^- event shape data. Similar results were obtained in Ref. [13].

4.1 Current jet thrust

In the case of the shape variables τ_Q or τ_E , the behaviour of the expression (4.6) for the transverse contribution $\mathcal{F}_T^{(\tau)}(x, \epsilon)$ as $\epsilon \rightarrow 0$ is found to be of the form

$$\mathcal{F}_T^{(\tau)}(x, \epsilon) \sim \mathcal{F}_T^{(\tau)}(x, 0) - 8\sqrt{\epsilon} q(x) , \quad (4.14)$$

while the longitudinal part $\mathcal{F}_L^{(\tau)}$ is less singular at $\epsilon = 0$. Thus from Eqs. (3.7), (4.1) and (4.7) we obtain the leading non-perturbative contribution

$$\delta \langle \tau \rangle \sim 4 \frac{A_1}{Q} . \quad (4.15)$$

The behaviour (4.14) at small ϵ follows from the fact that the derivative $\dot{\mathcal{F}}_T^{(\tau)}$ is dominated by the phase space boundary $z = 1 - \epsilon\xi/(1 - \xi)$:

$$\dot{\mathcal{F}}_T^{(\tau)}(x, \epsilon) \sim \epsilon \int_x^1 d\xi \int_0^1 dz \tau(\xi) C_{i,q}(\xi, z, 0) \delta(1 - z - \xi + \xi z - \epsilon\xi) q(x/\xi) . \quad (4.16)$$

From Table 1 and Eq. (4.5), on this boundary we have

$$\begin{aligned} \tau(\xi, z, 0) &= (1 - \xi)/\xi \quad \text{for } \xi > \xi_P , \\ &= (1 - z)/\xi \quad \text{for } \xi < \xi_P \end{aligned} \quad (4.17)$$

where $\xi_P = 1/(1 + \sqrt{\epsilon})$. Thus

$$\dot{\mathcal{F}}_T^{(\tau)}(x, \epsilon) \sim \int_x^{\xi_P} \frac{d\xi}{\xi} \epsilon \frac{1 + \xi^2}{(1 - \xi)^2} q\left(\frac{x}{\xi}\right) + \int_{\xi_P}^1 \frac{d\xi}{\xi} \frac{1 + \xi^2}{\xi} q\left(\frac{x}{\xi}\right) \sim 4\sqrt{\epsilon} q(x) , \quad (4.18)$$

in agreement with Eq. (4.14).

Numerical predictions for the mean value of the current jet thrust in ep scattering at $\sqrt{s} = 296 \text{ GeV}$ are shown in Fig. 4 as a function of Q for various values of x . The MRS A' parton distributions [26] were used, with the corresponding value $\Lambda_{\overline{\text{MS}}}^{(4)} = 231 \text{ MeV}$ in the two-loop expression for $\alpha_s(Q^2)$. The leading-order perturbative predictions given by Eq. (3.7) are shown by the dashed curves. For the power correction coefficient A_1 we used Eq. (4.12) with $\mu_R^2 = Q^2$, $\mu_I = 2 \text{ GeV}$ and $\bar{\alpha}_0(2 \text{ GeV}) = 0.52$, as in the fits to e^+e^- data, but we omitted the term of order α_s^2 because we are combining with only a first-order perturbative calculation in this paper. When the higher-order prediction becomes available,

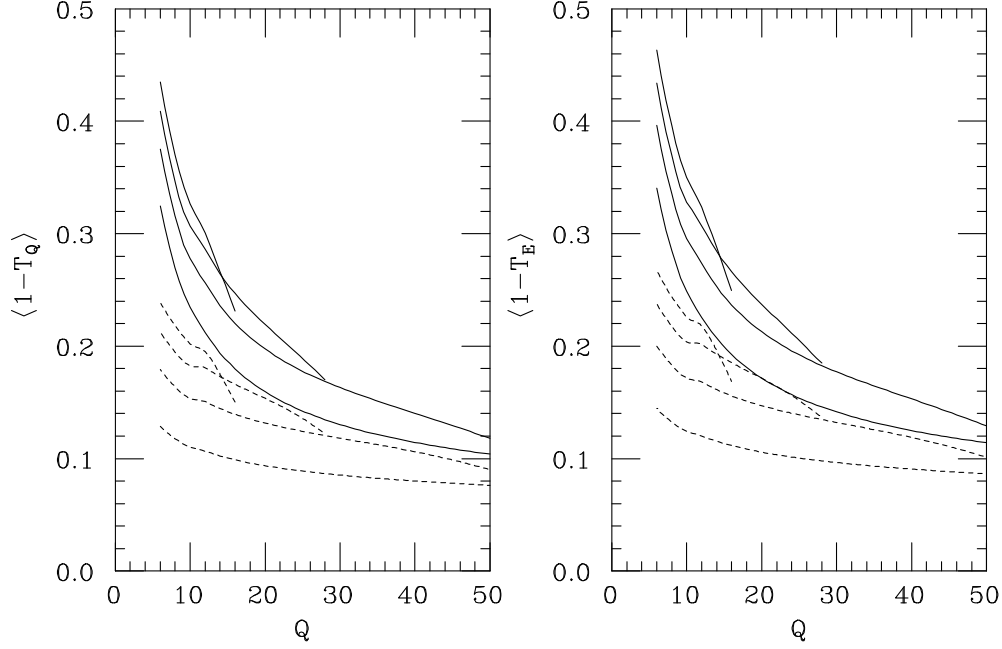


Figure 4: Predictions for the mean value of the current jet thrust in deep inelastic scattering. Left- and right-hand plots are for the two definitions (2.2) and (2.3), respectively. Dashed: leading-order perturbation theory. Solid: leading order plus leading power correction. In each case the four curves (top to bottom) are for $x = 0.003, 0.01, 0.03, 0.10$.

the $\mathcal{O}(\alpha_s^2)$ term in Eq. (4.12) should be included when estimating the power correction to it.

The resulting overall predictions are shown by the solid curves. We see that the estimated power correction is substantial, 20-30% at $Q = 50$ GeV and dominating below 15 GeV. There is significant x -dependence in the perturbative prediction, and large- x data ($x > 0.01$) are required to cover the region where the power correction is under control. With sufficient data in the range $Q = 15 - 50$ GeV, however, it should be possible to perform a two-parameter fit to determine α_s and $\bar{\alpha}_0$ from the average current jet thrust.

4.2 Current jet broadening

For the jet broadening B_Q or B_E we find a slightly different behaviour at small ϵ , namely

$$\mathcal{F}_T^{(B)}(x, \epsilon) \sim \mathcal{F}_T^{(B)}(x, 0) + 8\sqrt{\epsilon} (\ln \epsilon + c) q(x), \quad (4.19)$$

where c is a constant (probably x -independent) which we cannot determine reliably. This implies a non-perturbative correction of the form

$$\delta \langle B \rangle \sim 4 \frac{A_1}{Q} (\ln Q^2 - c - 2) - 4 \frac{A'_1}{Q}. \quad (4.20)$$

Since we do not know the value of c , we may as well absorb all the non-logarithmic terms into an unknown scale, Q_0 :

$$\delta \langle B \rangle = 8 \frac{A_1}{Q} \ln(Q/Q_0). \quad (4.21)$$

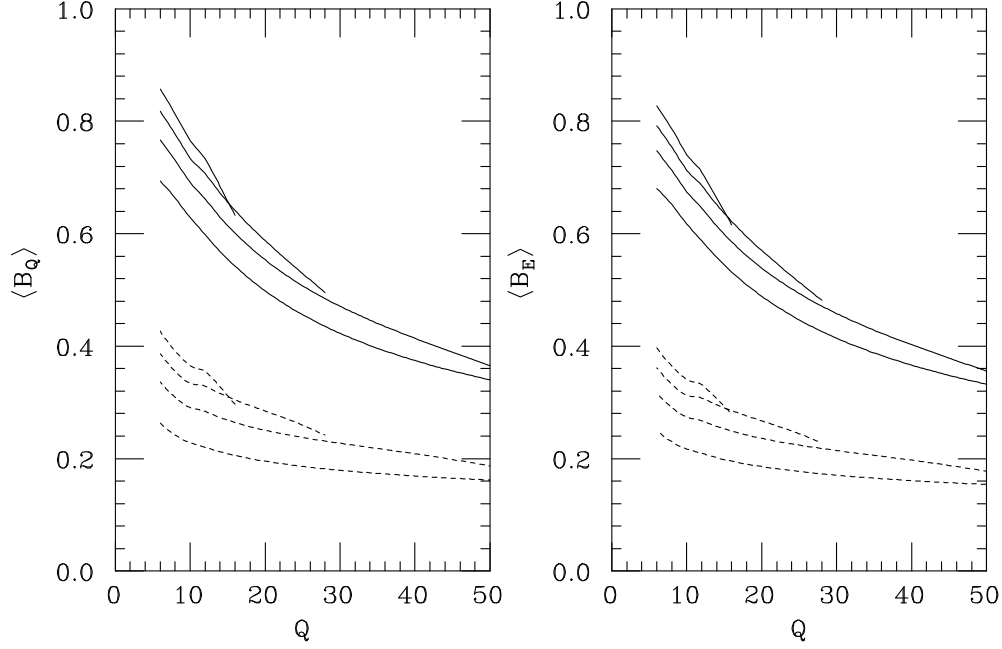


Figure 5: Predictions for the mean value of the current jet broadening in deep inelastic scattering. Left- and right-hand plots are for the two definitions (2.4) and (2.5), respectively. Curves as in Fig. 3.

We find that, in contrast to the situation for the thrust, the result (4.19) is only obtained when one includes the gluon mass explicitly in the definition of the jet broadening. This is because, unlike the thrust, the broadening vanishes on the phase-space boundary $z_{\perp} = 0$. If we neglect the gluon mass in the definition, this is not the case and an expression analogous to Eq. (4.16) is obtained, which gives

$$\dot{\mathcal{F}}_T^{(B)}(x, \epsilon) \sim \sqrt{\epsilon} \int_x^{\xi_P} \frac{d\xi}{1-\xi} \frac{\xi^2+1}{\xi} q\left(\frac{x}{\xi}\right) + 2\sqrt{\epsilon} \int_{\xi_P}^{1/(1+\epsilon)} \frac{d\xi}{1-\xi} \frac{\xi^2+1}{\xi} q\left(\frac{x}{\xi}\right). \quad (4.22)$$

We then find

$$\dot{\mathcal{F}}_T^{(B)}(\epsilon) \sim -3\sqrt{\epsilon} (\ln \epsilon + c), \quad (4.23)$$

corresponding to a coefficient of 6 instead of 8 in Eq. (4.21). Thus the correct form is obtained, but the full mass-dependence must be retained to compute the coefficient.

The fact that the magnitude of the leading power correction to the jet broadening is sensitive to the gluon mass-dependence in its definition suggests to us that the prediction for this shape variable is less reliable than that for the thrust. As pointed out in Ref. [9], shape variables are not fully inclusive with respect to the fragmentation of the gluon: their values for the ‘decay products’ of a timelike virtual gluon are not necessarily equal to those for a ‘real’ gluon of equivalent mass. In the case of the thrust, model studies suggest that the numerical effect of this on the leading power correction is small, but we expect it to be larger for variables that depend explicitly on the gluon mass.

Numerical predictions for the current jet broadening at HERA are shown in Fig. 5, using the same parameter values as before to compute A_1 and, for definiteness, $Q_0 = \mu_1 = 2$ GeV in Eq. (4.21). We see that the resulting power corrections are large. As we have stressed

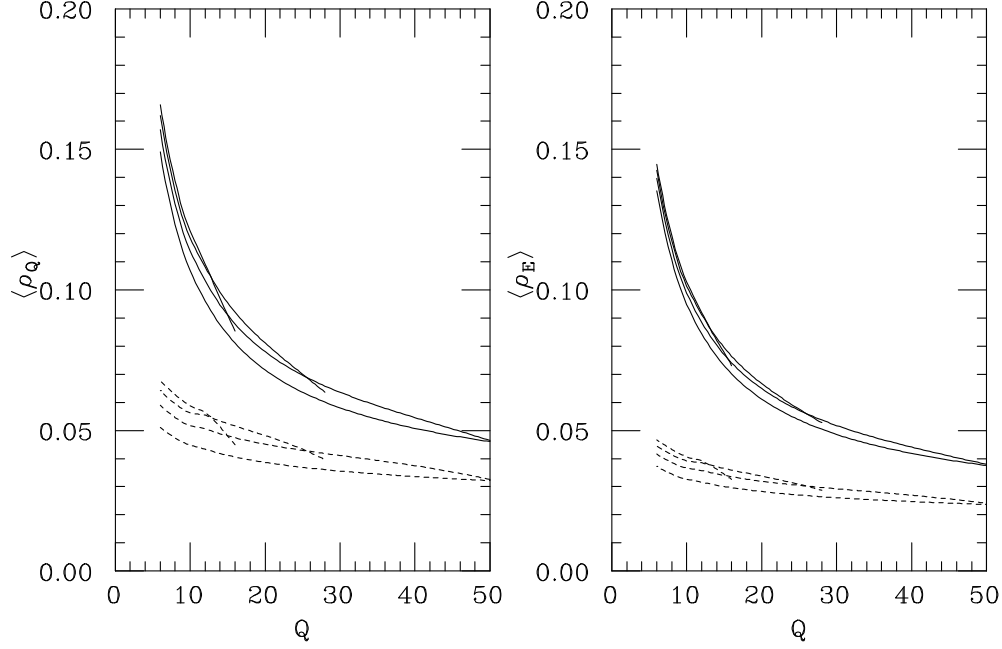


Figure 6: Predictions for the mean value of the current jet mass in deep inelastic scattering. Left- and right-hand plots are for the two definitions (2.6) and (2.9), respectively. Curves as in Fig. 3.

above, they are also more uncertain in this case, suggesting that jet broadening in DIS is not a good shape variable for α_s determinations.

4.3 Current jet mass

Next we consider the power corrections to the jet mass ρ_Q or ρ_E . We notice from Table 1 that there is no explicit gluon mass dependence in the definition of these variables, and there is no contribution outside the phase space region A.[†] Inside this region we have in fact $\rho_Q = \tau_Q$. Thus the jet mass receives a contribution from the second integral only in Eq. (4.18). This gives exactly one half of the correction to the thrust and so one finds that

$$\mathcal{F}_T^{(\rho)}(x, \epsilon) \sim \mathcal{F}_T^{(\rho)}(x, 0) - 4\sqrt{\epsilon} q(x) \quad (4.24)$$

at small ϵ , which implies a non-perturbative correction

$$\delta \langle \rho \rangle \sim 2 \frac{A_1}{Q}. \quad (4.25)$$

The numerical predictions for the current jet mass, shown in Fig. 6, suggest that this is a good variable for α_s determinations. The power correction is somewhat larger than that for the thrust, relative to the perturbative prediction (cf. Fig. 4), but there is less x dependence in the latter.

[†]There is a contribution ϵ in region C, but since this is analytic it does not contribute to the power correction.

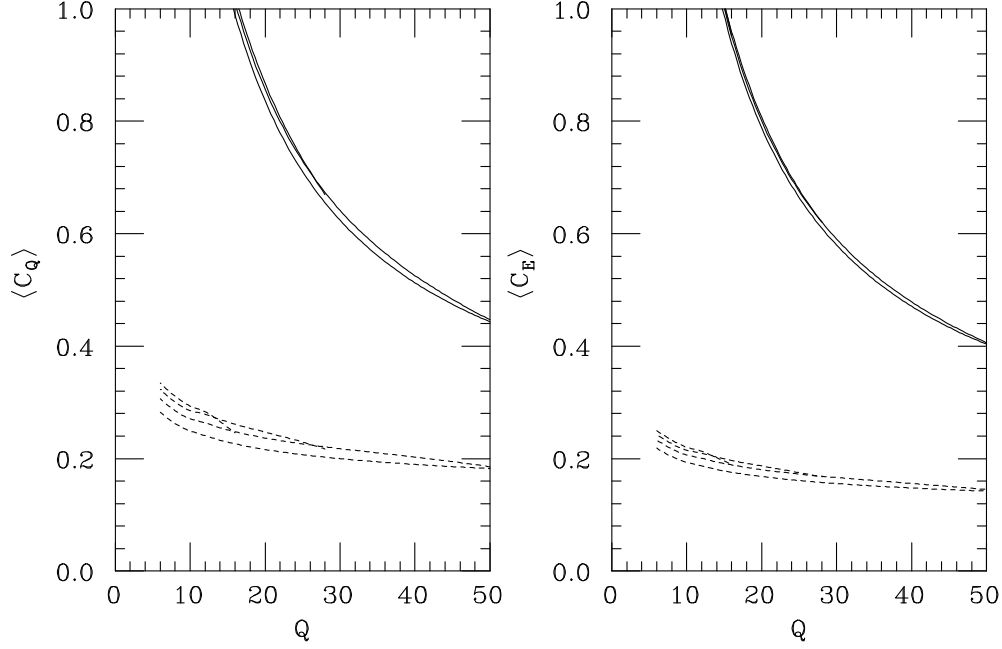


Figure 7: Predictions for the mean value of the C -parameter in deep inelastic scattering. Left- and right-hand plots are for the two definitions (2.7) and (2.9), respectively. Curves as in Fig. 3.

4.4 C -parameter

Finally we compute the power correction to C_Q or C_E . Here again we see from Table 1 that there is no contribution outside the phase space region A. However in this case the variable, unlike the jet mass, does depend explicitly on the gluon mass. From a full evaluation retaining this mass dependence we find the small- ϵ behaviour

$$\mathcal{F}_T^{(C)}(x, \epsilon) \sim \mathcal{F}_T^{(C)}(x, 0) - 24\pi\sqrt{\epsilon} q(x) , \quad (4.26)$$

corresponding to a leading non-perturbative contribution

$$\delta \langle C \rangle \sim 12\pi \frac{A_1}{Q} . \quad (4.27)$$

If one uses the massless gluon expression for C , one obtains

$$\dot{\mathcal{F}}_T^{(\tau)}(x, \epsilon) \sim 12\epsilon \int_{1/(1+\sqrt{\epsilon})}^{1/(1+\epsilon)} \frac{\xi^2 + 1}{\xi^2} \frac{(2\xi - 1)^2(1 - \xi)}{1 - \xi + \epsilon(1 - 2\xi)} \frac{d\xi}{(1 - \xi)^2 + \epsilon\xi(2\xi - 1)} \sim 6\pi\sqrt{\epsilon} , \quad (4.28)$$

which corresponds to one-half of the full result. We would argue again that this sensitivity to the gluon mass-dependence of the definition suggests that the prediction for the C -parameter is less reliable than that for the thrust and jet mass.

The numerical results, Fig. 7, show that the estimated power correction is very large in this case, dominating over the perturbative prediction even at $Q = 50$ GeV. The size and uncertainty in the correction suggest that, like the jet broadening, the C -parameter is not a good variable for determining α_s .

5 Summary

In this paper we have investigated several infrared-safe variables which characterize the shapes of DIS final states in the current hemisphere of the Breit frame, where one avoids as far as possible complications associated with the target remnant. We have presented numerical predictions to leading order in perturbation theory, together with estimates of leading non-perturbative power corrections, which are predicted to be proportional to $1/Q$, modulo logarithmic Q -dependence. The assumption of an approximately universal low-energy effective coupling allowed us to relate the magnitudes of the corrections to those in e^+e^- annihilation. We found that they are expected to be largest, and most uncertain, for the current jet broadening and C -parameter, and so these observables are probably not suitable for determination of the perturbative strong coupling α_s . The current jet thrust and mass should have power corrections that are smaller and under better control. When higher-order predictions for these quantities are available, our predictions of the power corrections can also be refined, and it should be possible to measure both α_s and the relevant non-perturbative parameter, $\bar{\alpha}_0(\mu_1)$ in Eq. (4.12), from these quantities.

Acknowledgements

M.D. acknowledges the financial support of Trinity College, Cambridge. We thank S. Catani, Yu.L. Dokshitzer, G. Marchesini, H.-U. Martyn and E. Mirkes for helpful conversations.

References

1. H1 Collaboration, T. Ahmed et. al., *Phys. Lett.* **346B** (1995) 415; ZEUS Collaboration, M. Derrick et al., *Phys. Lett.* **363B** (1995) 201.
2. J.G. Körner, E. Mirkes and G. Schuler, *Int. J. Mod. Phys.* **A4** (1989) 1781; T. Brodtkorb, J.G. Körner, E. Mirkes, and G. Schuler, *Zeit. Phys.* **C44** (1989) 415; T. Brodtkorb and J.G. Körner, *Zeit. Phys.* **C54** (1992) 519; T. Brodtkorb and E. Mirkes, *Zeit. Phys.* **C66** (1995) 141; D. Graudenz *Phys. Lett.* **256B** (1992) 518, *Phys. Rev.* **D49** (1994) 3291.
3. S. Catani, Y.L. Dokshitzer and B.R. Webber, *Phys. Lett.* **285B** (1992) 291.
4. E. Mirkes and D. Zeppenfeld, *Acta Phys. Polon.* **B27** (1996) 1393, *Nucl. Phys. Proc. Suppl.* **51C** (1996) 273, TTP-96-30 [hep-ph/9608201], MADPH-96-961 [hep-ph/9609274].
5. S. Catani and M.H. Seymour, *Nucl. Phys.* **B485** (1997) 291, CERN-TH/96-239 [hep-ph/9609237], CERN-TH/96-240 [hep-ph/9609521].
6. B.R. Webber, *Phys. Lett.* **339B** (1994) 148.
7. Yu.L. Dokshitzer and B.R. Webber, *ibid.* **352B** (1995) 451.
8. Yu.L. Dokshitzer, G. Marchesini and B.R. Webber, *Nucl. Phys.* **B469** (1996) 93.

9. P. Nason and M.H. Seymour, *Nucl. Phys.* **B454** (1995) 291.
10. G.P. Korchemsky and G. Sterman, in *Proc. 30th Rencontres de Moriond, Meribel-les-Allues, France, 1995* [hep-ph/9505391];
R. Akhoury and V.I. Zakharov, *Phys. Lett.* **357B** (1995) 646, *Nucl. Phys.* **B465** (1996) 295; V.M. Braun, NORDITA-96-65P [hep-ph/9610212]; M. Beneke, SLAC-PUB-7277 [hep-ph/9609215].
11. For reviews and classic references see V.I. Zakharov, *Nucl. Phys.* **B385** (1992) 452 and A.H. Mueller, in *QCD 20 Years Later*, vol. 1 (World Scientific, Singapore, 1993).
12. G. Grunberg, *Phys. Lett.* **372B** (1996) 121, CPTH-PC463-0896 [hep-ph/9608375];
D.V. Shirkov and I.L. Solovtsov, Dubna preprint, April 1996 [hep-ph/9604363].
13. DELPHI Collaboration, P. Abreu et al., *Zeit. Phys.* **C73** (1997) 229.
14. M. Dasgupta and B.R. Webber, *Nucl. Phys.* **B484** (1997) 247;
M. Beneke, V.M. Braun and L. Magnea, SLAC-PUB-7274 [hep-ph/9609266], CERN-TH/96-362 [hep-ph/9701309].
15. E. Stein, M. Meyer-Hermann, L. Mankiewicz and A. Schäfer, *Phys. Lett.* **376B** (1996) 177; M. Meyer-Hermann, M. Maul, L. Mankiewicz, E. Stein and A. Schäfer, *Phys. Lett.* **383B** (1996) 463, *ibid.* **393B** (1997) 487 (E); M. Maul, E. Stein, A. Schäfer and L. Mankiewicz, TUM-T39-96-29 [hep-ph/9612300];
M. Dasgupta and B.R. Webber, *Phys. Lett.* **382B** (1996) 273.
16. B.R. Webber in *Proc. Workshop on Deep Inelastic Scattering and QCD, Paris, 1995* [hep-ph/9510283].
17. K.H. Streng, T.F. Walsh and P.M. Zerwas, *Zeit. Phys.* **C2** (1979) 237.
18. R.D. Peccei and R. Rückl, *Nucl. Phys.* **B162** (1980) 125.
19. L.V. Gribov, Yu.L. Dokshitzer, S.I. Troyan and V.A. Khoze, *Sov. Phys. JETP* **68** (1988) 1303.
20. ZEUS Collaboration, M. Derrick et al., *Zeit. Phys.* **C67** (1995) 93;
H1 Collaboration, S. Aid et al., *Nucl. Phys.* **B445** (1995) 3.
21. S. Catani, G. Turnock and B.R. Webber, *Phys. Lett.* **295B** (1992) 269.
22. R.K. Ellis, D.A. Ross and A.E. Terrano, *Nucl. Phys.* **B178** (1981) 421.
23. M. Beneke, V.M. Braun and V.I. Zakharov, *Phys. Rev. Lett.* **73** (1994) 3058;
P. Ball, M. Beneke and V.M. Braun, *Nucl. Phys.* **B452** (1995) 563;
M. Beneke and V.M. Braun, *Nucl. Phys.* **B454** (1995) 253.
24. M.A. Shifman, A.I. Vainshtein and V.I. Zakharov, *Nucl. Phys.* **B147** (1979) 385, 448, 519;
Vacuum Structure and QCD Sum Rules: Reprints, ed. M.A. Shifman (North-Holland, 1992: Current Physics, Sources and Comments, v. 10).
25. S. Catani, G. Marchesini and B.R. Webber, *Nucl. Phys.* **B349** (1991) 635.
26. A.D. Martin, R.G. Roberts and W.J. Stirling, *Phys. Rev.* **D50** (1994) 6734.